A lipomannan with strong TLR-2 dependant pro-inflammatory activity in Saccharothrix aerocolonigenes

Kevin J. C. Gibson, M. Gilleron, P. Constant, B. Sichi, G. Puzo, Gurdyal S. Besra, J. Nigou

THE JOURNAL OF BIOLOGICAL CHEMISTRY
Vol. 280, No. 31, Issue of August 5, pp. 28347–28356, 2005
Printed in U.S.A.

A Lipomannan Variant with Strong TLR-2-dependent Pro-inflammatory Activity in *Saccharothrix aerocolonigenes**

Received for publication, May 19, 2005
Published, JBC Papers in Press, June 14, 2005, DOI 10.1074/jbc.M505498200

Kevin J. C. Gibson‡§, Martine Gilleron¶, Patricia Constant¶, Bénédicte Sichi¶, Germain Puzo¶, Gurdyal S. Besra‡‖, and Jérôme Nigou¶**

From the ‡School of Bioscience, The University of Birmingham, Edgbaston, Birmingham B15 2TT, United Kingdom, the ¶Department of Molecular Mechanisms of Mycobacterial Infections, Institut de Pharmacologie et de Biologie Structurale, CNRS, Unité Mixte de Recherche 5089, 205 Route de Narbonne, 31077 Toulouse cedex 4, France

Lipomannans (LMs) are powerful pro-inflammatory lipoglycans found in mycobacteria and related genera, however the molecular bases of their activity are not fully understood. We report here the isolation and the structural and functional characterization of a new lipomannan variant present in the *Pseudonocardineae*, *Saccharothrix aerocolonigenes*, designated SaeLM. Using a range of chemical degradations, NMR experiments, and mass spectrometry analyses, SaeLM revealed a mannosylphosphatidyl-*myo*-inositol (MPI) anchor glycosylated by an original carbohydrate structure whereby an (α1→6)-Man*p* backbone is substituted at >80% of the *O*-2 position by side chains composed of Man*p*-(α1→2)-Man*p*-(α1→. Matrix-assisted laser desorption ionization time-of-flight mass spectrometry analysis indicated a distribution of SaeLM glyco-forms ranging from 19 to 61 Man*p* units, which centered on species containing 37 or 40 Man*p* units. SaeLM induced a Toll-like receptor 2 (TLR-2)-dependent production of tumor necrosis factor-α (TNF-α) by human THP-1 monocyte/macrophage cell lines and interestingly was found to be the strongest inducer of this pro-inflammatory cytokine when compared with other LAM/LM-like molecules. We previously established that a linear (α1→6)-Man*p* chain, linked to the MPI anchor, is sufficient in providing pro-inflammatory activity. We demonstrate here that by adding side chains and increasing their size, one may potentiate this activity. These findings should enable a better understanding of the structure/function relationships of TLR-2-dependent lipoglycan signaling.

Lipomannan (LM)[1] and lipoarabinomannan (LAM) are related powerful immunomodulatory lipoglycans found in mycobacterial cell walls (1–5). Their structures originate from a phosphatidyl-*myo*-inositol (MPI) anchor, which is mannosylated to generate LM (4, 6) and further arabinosylated to give LAM. The non-reducing termini of the arabinosyl side chains can be substituted by capping motifs, yielding to the classification of LAM into three families. LAM from slow growing mycobacteria bearing mannose caps, *i.e.* mono- or (α1→2)-di- or tri-mannoside units, are designated as ManLAM. In contrast, LAM from fast growing mycobacteria capped by phospho-*myo*-inositol units or not capped at all are termed PILAM and AraLAM, respectively (4). LAM and LM exhibit a broad spectrum of immunomodulatory activities, including the ability to modulate the production of macrophage-derived Th1 pro-inflammatory cytokines, most commonly TNF-α and IL-12. For example, ManLAM are able to inhibit the LPS-induced production of IL-12 and TNF-α (7, 8). So, ManLAM contributes, via an immunosuppressive effect, to the persistence of slow-growing mycobacteria in the human reservoir. ManLAM anti-inflammatory activity has also been shown to require the interaction of ManLAM with the mannose receptor and/or dendritic cell-specific intercellular adhesion molecule-3 grabbing non-integrin via the mannose capping motifs (8–10). In contrast, PILAM are able to induce the release of a variety of pro-inflammatory cytokines through the activation of Toll-like receptors 2 (TLR-2) (11–13). This activity is likely to require PI caps, because AraLAM does not show any activity (14). Early studies demonstrated that LM from *Mycobacterium* sp. induce expression of pro-inflammatory cytokines (15). A set of recent reports have shown that LM from both pathogenic and non-pathogenic mycobacterial species, independent of their origin, were potent stimulators of TNF-α, IL-8, and IL-12 (16–18). Furthermore, LM was shown to activate macrophages in a TLR-2-dependent, and TLR-4- and TLR-6-independent manner (16–18). The ManLAM/LM balance might thus be a parameter influencing the net immune response against mycobacteria. Indeed, according to their activity, lipoglycans are therefore likely to favor either the persistence or the killing of the corresponding mycobacteria (3). Induction of a protective pro-inflammatory response via TLR signaling should be to the benefit of the host (19–21), whereas stimulation of anti-inflammatory response via mannose receptor or dendritic cell-specific intercellular adhesion molecule-3 grabbing non-integrin should be to the benefit of the pathogen (3, 10).

* This work was supported in part by grants from the CNRS (France) (to G. P.). The costs of publication of this article were defrayed in part by the payment of page charges. This article must therefore be hereby marked "*advertisement*" in accordance with 18 U.S.C. Section 1734 solely to indicate this fact.

§ Present address: Servier Laboratories Ltd., Gallions, Wexham Springs, Wexham, Slough SL3 6RJ, UK.

‖ Supported as a Lister Institute-Jenner Research Fellow and by grants from the Medical Research Council (UK) (Grant G0200510) and the Wellcome Trust (Grant 058972).

** To whom correspondence should be addressed: Tel: 33-561-175554; Fax: 33-561-175994; E-mail: jerome.nigou@ipbs.fr.

[1] The abbreviations used are: LM, lipomannan; Ara*f*, arabinofuranose; AraLAM, non-capped lipoarabinomannan; dSaeLM, deacylated *S. aerocolonigenes* lipomannan; GC, gas chromatography; HMBC, heteronuclear multiple bound correlation spectroscopy; HMQC, heteronuclear multiple quantum correlation spectroscopy; HOHAHA, homonuclear Hartmann-Hahn spectroscopy; IL, interleukin; LAM, lipoarabinomannan; mahTpaLAM, mild acidic hydrolyzed TpaLAM; MALDI-TOF, matrix assisted laser desorption ionization-time of flight; Man*p*, mannopyranose; ManLAM, LAM with mannosyl caps; MPI, mannosylphosphatidyl-*myo*-inositol; PILAM, LAM with phosphoinositide caps; PIM, phosphatidyl-*myo*-inositol mannoside; ROESY, rotating Overhauser and exchange spectroscopy; SaeLM, *S. aerocolonigenes* lipomannan; t, terminal; TLR, Toll-like receptor; TNF-α, tumor necrosis factor α; TpaLAM, *T. paurometabola* lipoarabinomannan; BCG, bacillus Calmette-Guerin; nOe, nuclear Overhauser effect.

The molecular bases of LM/LAM pro- *versus* anti-inflammatory activities are not yet fully understood. Nevertheless, it seems clear that LM or the lipomannan moiety of LAM bear the intrinsic capacity to induce the production of TNF-α and IL-12 (16, 22). However, the presence of the arabinan moiety on LAM inhibits the pro-inflammatory activity, presumably by masking the mannan core (23, 24) and thus limiting its accessibility to the TLR (16, 22). Also, the type of capping motifs may then direct LAM activity toward a pro- (PILAM) or anti-(ManLAM) inflammatory activity (3).

Further insights into deciphering these complex molecular interactions could benefit from the structural and functional characterization of LAM variants. Indeed, lipoglycans are not restricted to members of the mycobacteria, and a number of non-mycobacterial lipoglycans have been isolated and characterized in several actinomycete genera, including *Rhodococcus* (25, 26), *Gordonia* (27), *Amycolatopsis* (28), *Corynebacterium* (29), and most recently *Turicella* (30) and *Tsukamurella* (22). In the latter study, we demonstrated that LAM from *Tsukamurella paurometabola* (TpaLAM) possesses a similar structural prototype when compared with mycobacterial LAM, with distinct mannan and arabinan domains, yet had weak biological activity (22); however, upon chemical degradation of the arabinan domain, the resulting lipomannan moiety elicited a powerful pro-inflammatory response as previously demonstrated with ManLAM (16). Interestingly, the TpaLAM lipomannan moiety is composed of a linear (α1→6)-Man*p* chain linked to the MPI anchor demonstrating that this structure alone is sufficient in providing pro-inflammatory activity, and that, importantly, the branched t-Man*p* units are not necessarily required (22).

In the present study we report the isolation, structural, and functional characterization of a LM molecule from the *Pseudonocardineae*, *Saccharothrix aerocolonigenes* (31). The investigation revealed an original structure, and, furthermore, we demonstrate that LM possessed potent pro-inflammatory activity. As such, the structure/function relationship of the lipomannan is discussed, enabling further insights into the molecular basis of lipoglycan-mediated inflammatory responses.

MATERIALS AND METHODS

Bacteria and Growth Conditions—*S. aerocolonigenes*, type strain DSM 40034 (*S. aerocolonigenes* subsp. *aerocolonigenes*, recently renamed as *Lechevaliera aerocolonigenes* (32)) was purchased from DSMZ, Germany. It was routinely grown at 30 °C in GYM streptomyces medium, which contained 4 g of glucose, 4 g of yeast extract, and 10 g of maltose per liter of deionized water supplemented with 0.05% (w/v) Tween 80. Cells were grown to late log phase and harvested by centrifugation, washed, and lyophilized.

Purification of SaeLM—Purification procedures were adapted from protocols established for the extraction and purification of mycobacterial lipoglycans (33, 34). Briefly, the cells were delipidated at 60 °C by mixing in $CHCl_3$/CH_3OH (1:1, v/v) overnight. The organic extract was removed by filtration, and the delipidated biomass was resuspended in deionized water and disrupted by sonication (MSE Soniprep, 12 micro amplitude, 60 s on then 90 s off for 10 cycles, on ice). The cellular glycans and lipoglycans were further extracted by refluxing the broken cells in 50% ethanol at 65 °C overnight. Contaminating proteins and glucans were removed by enzymatic degradation using protease and α-amylase treatments followed by dialysis. The resulting extract was resuspended in buffer A, 15% propan-1-ol in 50 mM ammonium acetate, and loaded onto an octyl-Sepharose CL-4B column (50 × 2.5 cm) and eluted with 400 ml of buffer A at 5 ml/h, enabling the removal of non-lipidic moieties. The retained lipoglycans were eluted with 400 ml of buffer B, 50% propan-1-ol in 50 mM ammonium acetate. The resulting lipoglycans were resuspended in buffer C, 0.2 M NaCl, 0.25% sodium deoxycholate (w/v), 1 mM EDTA, and 10 mM Tris, pH 8, to a final concentration of 200 mg/ml and loaded onto a Sephacryl S-200 HR column (50 × 2.5 cm) and eluted with buffer C at a flow rate of 5 ml/h. Fractions (1.25 ml) were collected and analyzed by SDS-PAGE followed by periodic acid-silver nitrate staining. The resulting lipoglycan fractions were pooled, dialyzed extensively against water, lyophilized, and stored at −20 °C.

Preparation of Deacylated SaeLM—Deacylated SaeLM (dSaeLM) was obtained by incubating 100 μg of SaeLM with 200 μl of 0.1 N NaOH for 2 h at 37 °C. The reaction was stopped by extensive dialysis against water.

MALDI/MS—The matrix used was 2,5-dihydroxybenzoic acid at a concentration of 10 μg/μl, in a mixture of water/ethanol (1:1, v/v). 0.5 μl of SaeLM, at a concentration of 10 μg/μl, was mixed with 0.5 μl of the matrix solution. Analyses were performed on a Voyager DE-STR MALDI-TOF instrument (PerSeptive Biosystems, Framingham, MA) using linear mode detection. Mass spectra were recorded in the negative mode using a 300-ns time delay with a grid voltage of 95% of full accelerating voltage (24 kV) and a guide wire voltage of 0.05%. The mass spectra were mass assigned using external calibration.

Fatty Acid Analysis—200 μg of SaeLM was deacylated using strong alkaline hydrolysis (200 μl of 1 M NaOH at 110 °C for 2 h). The reaction mixture was neutralized with HCl, and the liberated fatty acids were extracted three times with chloroform and, after drying under nitrogen, were methylated using three drops of 10% (w/w) BF_3 in methanol (Fluka) at 60 °C for 5 min. The reaction was stopped by the addition of water, and the fatty acid methyl esters were extracted three times with chloroform. After drying, the fatty acid methyl esters were solubilized in 10 μl of pyridine and trimethyl-silylated using 10 μl of hexamethyldisilazane and 5 μl of trimethylchlorosilane at room temperature for 15 min. After drying under a stream of nitrogen, the fatty acid derivatives were solubilized in cyclohexane before analysis by gas chromatography (GC) and gas chromatography-mass spectrometry (GC/MS).

Glycosidic Linkage Analysis—Glycosyl linkage composition was performed according to the modified procedure of Ciucanu and Kerek (35). The per-*O*-methylated SaeLM was hydrolyzed using 500 μl of 2 M trifluoroacetic acid at 110 °C for 2 h, reduced using 350 μl of a 10 mg/ml solution of $NaBD_4$ (NH_4OH 1 M/C_2H_5OH, 1:1, v/v), and per-*O*-acetylated using 300 μl of acetic anhydride for 1 h at 110 °C. The resulting alditol acetates were solubilized in cyclohexane before analysis by GC and GC/MS.

NMR Spectroscopy—NMR spectra were recorded on a Bruker DMX-500 spectrometer equipped with a double resonance (^{1}H/X)-BBi z-gradient probe head. SaeLM (20 mg) was exchanged in D_2O (D, 99.97% from Euriso-top, Saint-Aubin, France), with intermediate lyophilization, then re-dissolved in 0.4 ml of Me_2SO-d6 (D, 99.8% from Euriso-top), and analyzed in 200- × 5-mm 535-PP NMR tubes at 343 K. Data were processed on a Bruker-X32 workstation using the xwinnmr program. Proton and carbon chemical shifts are expressed in ppm and referenced relative to internal Me_2SO signals at δ_H 2.52 and δ_C 40.98. The one-dimensional (1D) proton (^{1}H) spectra were recorded using a 90° tipping angle for the pulse and 1 s as recycle delay between each of the 387 acquisitions of 1.64 s. The spectral width of 3,064 Hz was collected in 16,000 complex points that were multiplied by a Gaussian function (LB = −1, GB = 0.4) prior to processing to 32,000 real points in the frequency domain. After Fourier transformation, the spectra were baseline corrected with a fourth order polynomial function. The 1D ^{31}P spectrum was measured at 202.46 MHz at 343 K and phosphoric acid (85%) was used as external reference (δ_P 0.0). The spectral width of 20 kHz was collected in 16,000 complex points that were multiplied by an exponential function (LB = 1 Hz) prior to processing to 32,000 real points in the frequency domain. The scan number was 256. Two-dimensional (2D) spectra were recorded without sample spinning, and data were acquired in the phase-sensitive mode using the time-proportional phase increment method. The 2D ^{1}H-^{13}C Heteronuclear Multiple Quantum Correlation (HMQC) and ^{1}H-^{31}P HMQC-HOHAHA were recorded in the proton-detected mode with a Bruker 5-mm ^{1}H broad band tunable probe with reverse geometry. The globally optimized alternating-phase rectangular pulses (GARP) sequence (36) at the carbon or phosphorus frequency was used as a composite pulse decoupling during acquisition. The ^{1}H-^{13}C HMQC spectrum was obtained according to Bax and Subramanian pulse sequence (37). Spectral widths of 25,154 Hz in ^{13}C and 2200 Hz in ^{1}H dimensions were used to collect a 2,048 × 512 (time-proportional phase increment) point data matrix with 56 scans/t1 value expanded to 4,096 × 1,024 by zero filling. The relaxation delay was 1 s. A sine bell window shifted by π/2 was applied in both dimensions. A ^{1}H-^{13}C HMBC spectrum was obtained using the Bax and Summers pulse sequence (38). Spectral widths of 25,154 Hz in ^{13}C and 3,064 Hz in ^{1}H dimensions were used to collect a 2,048 × 480 (time-proportional phase increment) point data matrix with 80 scans/t1 value expanded to 4,096 × 1,024 by zero filling. The relaxation delay was 1 s. A sine bell window shifted by π/2 was applied in both dimensions. A ^{1}H-^{31}P HMQC-HOHAHA spectrum was obtained using the Lerner and

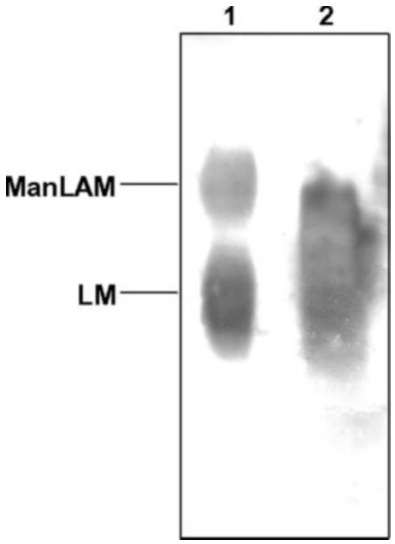

FIG. 1. **SDS-PAGE analysis of *S. aerocolonigenes* lipoglycan.** *Lane 1*, *M. tuberculosis* ManLAM and LM (*top* and *bottom bands*, respectively); *lane 2*, *S. aerocolonigenes* lipoglycan.

Bax pulse sequence (39). Spectral widths of 1,620 Hz in ^{31}P and 3,064 Hz in ^{1}H dimensions were used to collect a 2,048 × 80 (time-proportional phase increment) point data matrix with 16 scans/t1 value expanded to 4,096 × 1,024 by zero filling. The relaxation delay was 1 s. A sine bell window shifted by $\pi/2$ was applied in both dimensions. The 2D ^{1}H-^{1}H HOHAHA spectrum was recorded using a MLEV-17 mixing sequence of 110 ms (40). The spectral width was 3,064 Hz in both F_2 and F_1 dimensions. 450 spectra of 4,096 data points with 24 scans/t1 increment were recorded. The 2D ^{1}H-^{1}H ROESY spectrum was acquired at a mixing time of 300 ms (41). The spectral width was 3,064 Hz in both dimensions. 512 spectra of 2,048 data points with 24 scans/t1 increment were recorded.

TNF-α Production by Macrophages—A THP-1 monocyte/macrophage human cell line was maintained in continuous culture with RPMI 1640 medium (Invitrogen), 10% fetal calf serum (Invitrogen) in an atmosphere of 5% CO_2 at 37 °C, as non-adherent cells. Purified native or modified SaeLM as well as the other stimuli were added in duplicate or triplicate to monocyte/macrophage cells (5 × 10^5 cells/well) in 24-well culture plates and then incubated for 20 h at 37 °C. Stimuli were previously incubated for 1 h at 37 °C in the presence or absence of 10 μg/ml polymyxin B (Sigma) known to inhibit the effect of (contaminating) LPS (12). To investigate the TLR dependence of TNF-α-inducing SaeLM activity, monoclonal anti-TLR-2 (clone TL2.1, eBioscience) or anti-TLR-4 (clone HTA125, Serotec) antibodies or an IgG2a isotype control (clone eBM2a, eBioscience) at concentrations of 10 and 20 μg/ml were added together with SaeLM to THP-1 cells. Supernatants from THP-1 cells were assayed for TNF-α by sandwich enzyme-linked immunosorbent assay using commercially available kits and according to the manufacturer's instructions (R&D Systems). LPS was from *Escherichia coli* 055:B5 (Sigma), ManLAM and LM were from *Mycobacterium bovis* BCG, and mahTpaLAM was from *T. paurometabola* (22).

RESULTS

A lipoglycan that migrated in SDS-PAGE between *Mycobacterium tuberculosis* ManLAM and LM was purified from *S. aerocolonigenes* (Fig. 1). The lipoglycan contained mannose as the sole carbohydrate, *myo*-inositol, glycerol, and fatty acids. The predominant fatty acids identified by GC were 14-methylpentadecanoic (iC16:0) (33%), palmitic (C16:0) (20%), and octadecenoic (C18:1) (33%), with smaller amounts of stearic (C18:0) (6%), and various isomers of heptadecanoic (C17) (altogether 8%) acids. The lipoglycan exhibited the same basic components of a structure related to mycobacterial LM and was subsequently termed SaeLM.

Mannan Backbone—The ^{1}H NMR anomeric region of SaeLM was dominated by three signals at δ 5.03 (Ia_1), δ 4.98 (IIa_1), and δ 4.84 ($IIIa_1$), with nearly identical intensities (Fig. 2*A*). As revealed by the ^{1}H-^{13}C HMQC spectrum, their corresponding anomeric carbons resonate at δ 101.4 (Ia_1), δ 102.4 (IIa_1), and δ 99.4 ($IIIa_1$) (Fig. 2*E*). Anomeric proton and carbon resonances of the different spin systems were assigned from 2D ^{1}H-^{13}C HMQC (Fig. 2, *D* and *E*) and HMBC (Fig. 2*C*) and ^{1}H-^{1}H HOHAHA (Fig. 3*C*) and ROESY (Fig. 3*D*) experiments based on our previous studies with mycobacterial LAMs and LMs (42, 43). The assignments are summarized in Table I. Spin systems Ia, IIa, and IIIa were unambiguously assigned to 2-α-Man*p*, t-α-Man*p*, and 2,6-α-Man*p*, respectively, in agreement with per-*O*-methylation data. The α-anomeric configuration was demonstrated through the magnitude of their $^{1}J_{H1,C1}$ coupling constants determined as 174, 171, and 169 Hz for spin systems Ia, IIa, and IIIa, respectively (α-*O*-Me-Man*p*: $^{1}J_{H\text{-}1,C\text{-}1}$ 170 Hz; β-*O*-Me-Man*p*: $^{1}J_{H\text{-}1,C\text{-}1}$ 161 Hz (44)). The pyranose ring was deduced from their $\delta_{C\text{-}5}$ at 74.7, 73.1, and 74.2, respectively, and the presence on the ^{1}H-^{13}C HMBC spectrum (Fig. 2*C*) of cross-peaks between their H-1 and their respective C-5. ^{1}H and ^{13}C chemical shifts of spin system IIa (Table I) indicated an unsubstituted t-Man*p* unit (42, 43). Glycosylation at position 2 of 2-α-Man*p* (I) and 2,6-α-Man*p* (III) units was determined by the deshielding of their C-2 resonance at δ 77.0 and δ 77.8, respectively, as compared with the C-2 resonance of the unsubstituted t-α-Man*p* unit at δ 71.0 (Δδ 6.0 and 6.8 ppm, respectively) (Fig. 2*D* and Table I). Glycosylation at position 6 of 2,6-α-Man*p* (III) units was shown through the deshielding of the C-6 resonance at δ 66.0 as compared with the C-6 resonance of the unsubstituted t-α-Man*p* unit at δ 62.4 (Δδ 3.6 ppm) (Fig. 2*D* and Table I).

The sequence of these units was first investigated by ^{1}H-^{13}C HMBC NMR experiments (Fig. 2*C*). H-1 of 2-α-Man*p* (Ia_1) at δ 5.03 showed intracyclic connectivities with their C-2 at δ 77.0, C-3 at δ 71.6, and C-5 at δ 74.7. An additional intercyclic connectivity with C-2 of 2,6-α-Man*p* at δ 77.8 indicated that 2-α-Man*p* were linked at *O*-2 of 2,6-α-Man*p*. H-1 of t-α-Man*p* (IIa_1) at δ 4.98 showed intracyclic connectivities with their C-2 at δ 71.0, C-3 at δ 72.1, and C-5 at δ 73.1. An additional intercyclic connectivity with C-2 of 2-α-Man*p* at δ 77.0 indicated that t-α-Man*p* were linked at *O*-2 of 2-α-Man*p*. H-1 of 2,6-α-Man*p* ($IIIa_1$) at δ 4.84 showed intracyclic connectivities with their C-2 at δ 77.8, C-3 at δ 71.8, and C-5 at δ 74.2, respectively, and an intercyclic connectivity with their own C-6 at δ 66.0 establishing that 2,6-α-Man*p* are interconnected by (α1→6) linkage. Altogether the data indicated 2,6-α-Man*p* units were substituted at *O*-2 by the Man*p*-(α1→2)-Man*p*-(α1→ dimannoside motif. This was further confirmed by ^{1}H-^{1}H ROESY analysis (Fig. 3*D*). Indeed, H-1 of the 2-α-Man*p* unit (Ia_1) at δ 5.03 showed an intense inter-residue nOe contact with H-2 of 2,6-α-Man*p* unit ($IIIa_2$) at δ 3.81. H-1 of the t-α-Man*p* unit (IIa_1) at δ 4.98 showed an intense inter-residue nOe contact with H-2 of 2-α-Man*p* unit (Ia_2) at δ 3.88. H-1 of 2,6-α-Man*p* unit ($IIIa_1$) at δ 5.03 showed inter-residues nOe contacts with their own H-6 and H-6′ at δ 3.50 and δ 3.92, respectively.

Spin systems with weaker intensities were also present. Spin system IV characterized by $\delta_{H\text{-}1}$ 4.71 (Figs. 2*A* and 3*A*) and $\delta_{C\text{-}1}$ 99.4 (Fig. 2*E*) was attributed to 6-α-Man*p* unit (Table I). H-1 of 6-α-Man*p* (IV_1) showed, upon ^{1}H-^{13}C HMBC analysis, a connectivity with a carbon at δ 66.7, attributed to their own C-6 establishing that 6-α-Man*p* are interconnected by a (α1→6) linkage. Integration of ^{1}H NMR signals provided a ratio 2,6-α-Man*p*/6-α-Man*p* of 1.0/0.2, indicating that 83% of the (α1→6)-linked Man*p* units are substituted at *O*-2 positions by the Man*p*-(α1→2)-Man*p*-(α1→ dimannoside motif. Interestingly, the 2,6-α-Man*p* and 6-α-Man*p* units exhibited distinct C-6 resonances (Table I), with both H-1 units correlating with their own C-6 resonances in the HMBC spectrum (Fig. 2*C*). Taken

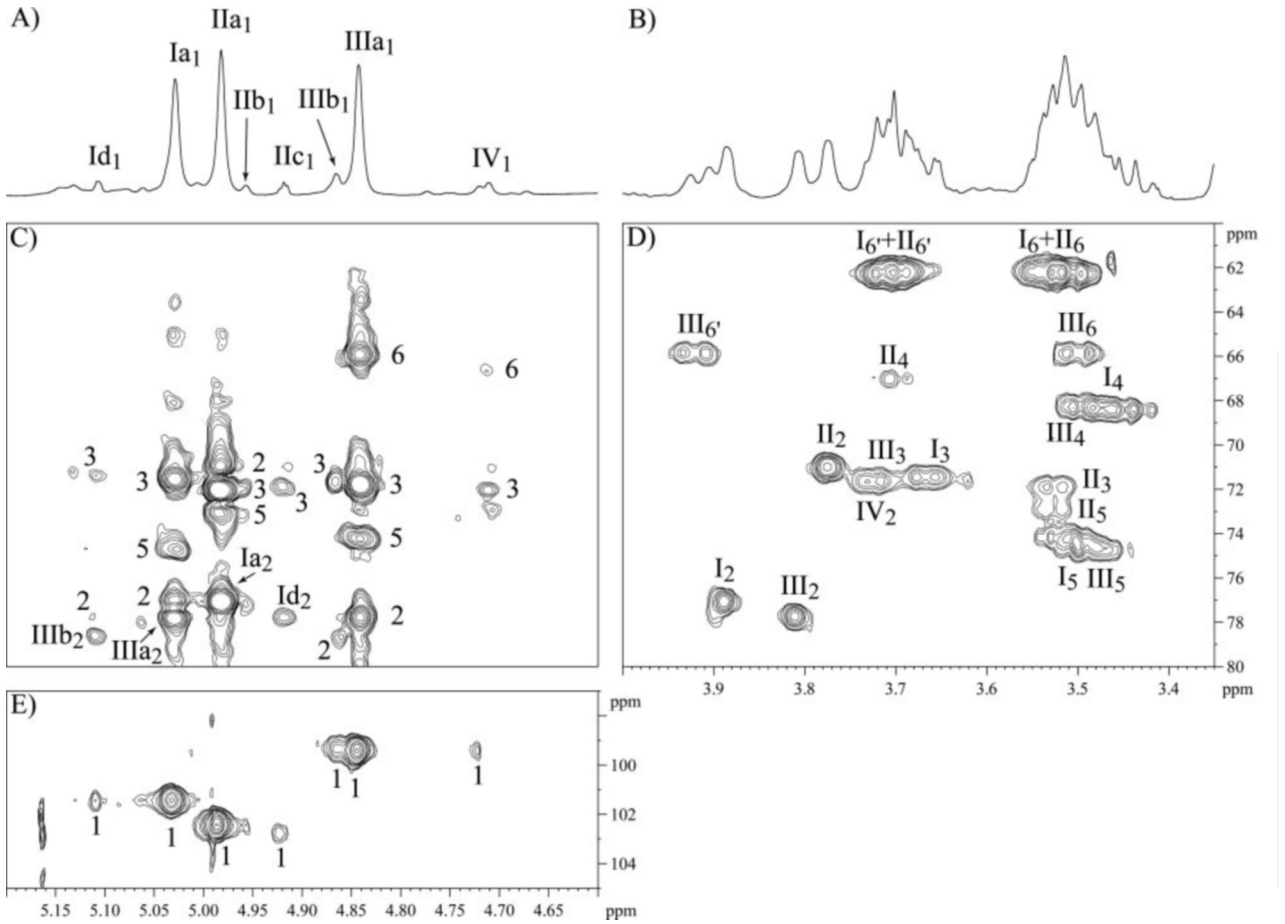

FIG. 2. **1D ^{1}H (*A* and *B*), 2D ^{1}H-^{13}C HMBC (*C*), and 2D ^{1}H-^{13}C HMQC (*D* and *E*) NMR spectra of SaeLM in Me_2SO-d6 at 343 K.** Expanded regions δ ^{1}H: 4.60–5.20 (*A*), δ ^{1}H: 3.35–4.00 (*B*), δ ^{1}H: 4.60–5.20, δ ^{13}C: 60–80 (*C*), δ ^{1}H: 3.35–4.00, δ ^{13}C: 60–80 (*D*), and δ ^{1}H: 4.60–5.20, δ ^{13}C: 97–105 (*E*) are shown. Glycosyl residues are labeled in *roman numerals*, and their carbons and protons are labeled with *Arabic numerals*. *I*, 2-α-Man*p*; *II*, t-α-Man*p*; *III*, 2,6-α-Man*p*; and *IV*, 6-α-Man*p*.

together, one may conclude that the 2,6-α-Man*p* and 6-α-Man*p* units form separate and distinct domains.

Spin systems Ib, -c, and -d characterized by $\delta_{H\text{-}1}$ 5.06, 5.08, and 5.11, respectively (Fig. 3*A*) and $\delta_{C\text{-}1}$ 101.4 (Fig. 2*E*) were attributed, by similarity to spin system Ia, as 2-α-Man*p* units (Table I). In a similar manner, spin systems IIb and -c, characterized by $\delta_{H\text{-}1}$ 4.96 and 4.92, respectively (Fig. 3*A*), and $\delta_{C\text{-}1}$ 102.5 and 102.8, respectively (Fig. 2*E*), were attributed to t-α-Man*p* units (Table I). Finally, spin systems IIIb and -c characterized by $\delta_{H\text{-}1}$ 4.86 and 4.87 (Fig. 3*A*) and $\delta_{C\text{-}1}$ 99.4 (Fig. 2*E*) were attributed to 2,6-α-Man*p* units (Table I). H-1 of the t-α-Man*p* unit (IIc_1) at δ 4.92 showed an intense inter-residue nOe contact with H-2 of 2-α-Man*p* unit (Id_2) at δ 3.90, whereas H-1 of these 2-α-Man*p* unit (Id_1) at δ 5.11 showed an intense inter-residue nOe contact with H-2 of 2,6-α-Man*p* unit ($IIIb_2$) at δ 3.79. As the main spin systems (Ia, IIa, and IIIa), these spin systems characterize the trisaccharide structure: Man*p*-(α1→2)-Man*p*-(α1→2)-[→6)]-Man*p*-(α1→. The linkage of these units was further confirmed by HMBC experiment (Fig. 2*A*). Indeed, H-1 of the t-α-Man*p* unit (IIc_1) at δ 4.92 showed an inter-residue correlation with C-2 of 2-α-Man*p* unit (Id_2) at δ 77.8, whereas H-1 of these 2-α-Man*p* units (Id_1) at δ 5.11 showed an inter-residue correlation with C-2 of the 2,6-α-Man*p* unit ($IIIb_2$) at δ 78.6. In a similar manner, H-1 of spin system Ic (Ic_1) at δ 5.08 showed an intense inter-residue nOe contact with H-2 of spin system IIIc ($IIIc_2$) at δ 3.76 characterizing the sequence →2)-Man*p*-(α1→2)-[→6)]-Man*p*-(α1→. No obvious correlations could be observed with the remaining low abundant spin systems either in the ROESY or HMBC experiments. Thus one may conclude that the trisaccharide motifs characterized by these spin systems are probably located at a specific site in the structure, for example at the beginning or the end of the mannan chain.

MPI Anchor—The presence and structure of the MPI anchor was first investigated by 1D ^{31}P and 2D ^{1}H-^{31}P NMR of SaeLM dissolved in Me_2SO at 343 K. The 1D ^{31}P showed four resonances at δ 1.83, 1.90, 3.58, and 3.83, in a ratio 1.0:1.0:1.4:1.8 indicative of the presence of different SaeLM acyl-forms (Fig. 4). As expected, in the 2D ^{1}H-^{31}P HMQC-HOHAHA experiment, each phosphorus resonance correlated with a complex set of signals attributed to protons of *myo*-inositol and glycerol (Fig. 5, *A* and *B*). Protons H-1 of *myo*-inositol and H-3 and H-3′ of glycerol were attributed using ^{1}H-^{31}P HMQC experimentation (data not shown; Table I). The attribution of the remaining *myo*-inositol and glycerol signals was resolved using literature data to compare chemical shifts and multiplicity, and further confirmed by ^{1}H-^{1}H HOHAHA experiments (Fig. 5*C* and Table I) (43, 45). Glycerol units with phosphates resonating at δ 1.83 and 1.90 corresponded to diacylglycerol units, as revealed by the deshielding of their H-2 proton at δ 5.12 (Fig. 5*A* and Table I). In contrast, Glycerol units linked to phosphates resonating at δ 3.58 and 3.83 did not show a deshielded H-2 proton, corresponding to 1-acyl-2-lysoglycerol units (Fig. 5*B* and Table I). These attributions were in agreement with the chemical shift ranges of the corresponding phosphorus atoms, phosphodiacylglycerols (high field) *versus* phosphomonoacylglycerols (low field) (45, 46). The *myo*-inositol units derived from the four phosphorus atoms showed very similar proton chemical shifts that indicated non-acylated units (Fig. 5, *A* and *B*, and

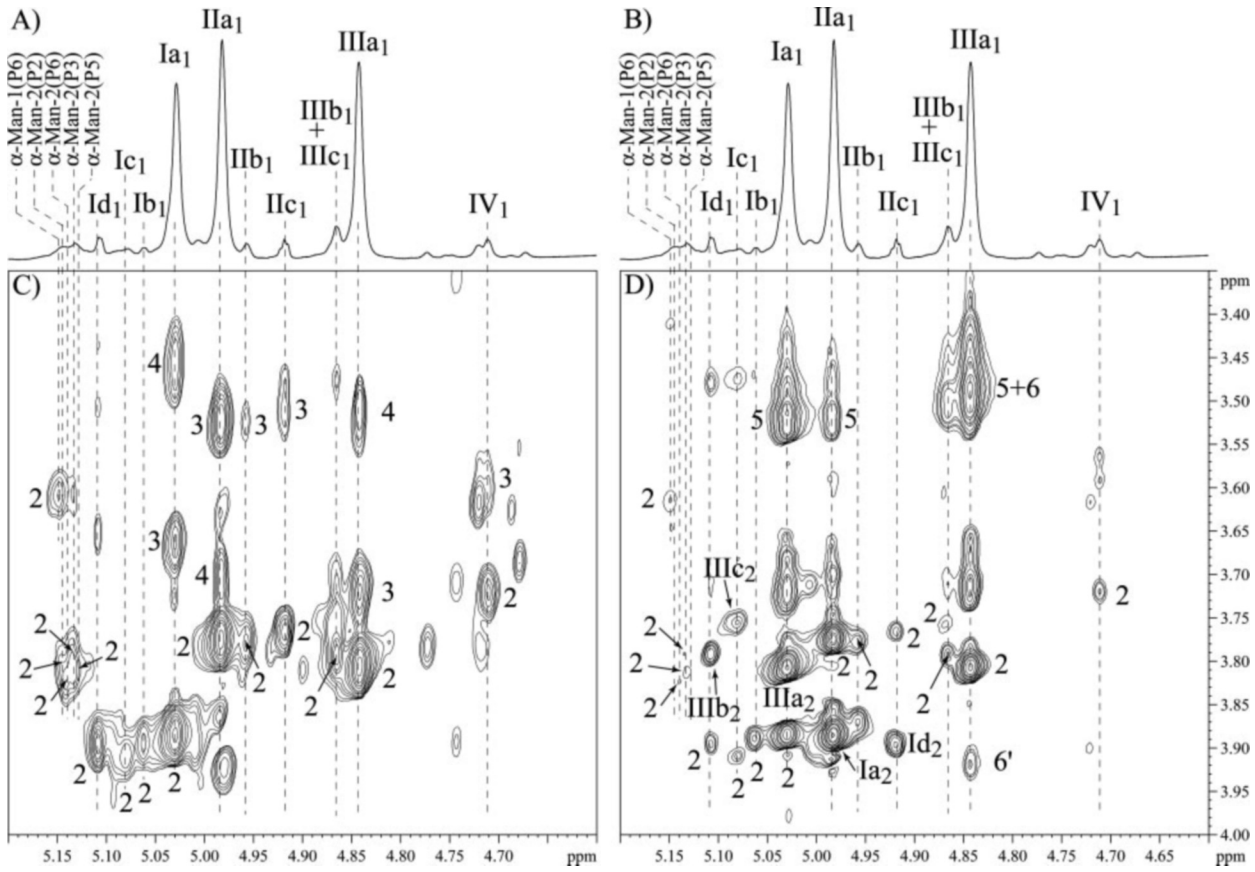

FIG. 3. **1D ^{1}H (*A* and *B*) and 2D ^{1}H-^{1}H HOHAHA τ_m 110 ms (*C*) and ROESY τ_m 300 ms (*D*) spectra of SaeLM in Me_2SO-d6 at 343 K.** Expanded regions (δ ^{1}H: 4.60–5.20 (*A* and *B*) and δ ^{1}H: 4.60–5.20, δ ^{1}H: 3.35–4.00 (*C* and *D*)) are shown. Glycosyl residues are labeled in *roman numerals*, and their carbons and protons are labeled with *Arabic numerals*. *I*, 2-α-Man*p*; *II*, t-α-Man*p*; *III*, 2,6-α-Man*p*; *IV*, 6-α-Man*p*; *α-Man-1*, α-Man*p* unit linked at *O*-6 of the *myo*-inositol; and *α-Man-2*, α-Man*p* unit linked at *O*-2 of the *myo*-inositol.

TABLE I

Proton and carbon chemical shifts of SaeLM

Chemical shifts were measured at 343 K in Me_2SO-d6 and are referenced relative to internal Me_2SO signals at δ_H 2.52 and δ_C 40.98.

Residue		Chemical shifts					
		H-1, C-1	H-2, C-2	H-3, C-3	H-4, C-4	H-5(/H-5′), C-5	H-6/H-6′, C-6
		ppm					
2-α-Man*p*	(I) a	5.03, 101.4	3.88, 77.0	3.66, 71.6	3.44, 68.5	3.52, 74.7	3.72/3.55–3.49[a], 62.4
	b	5.06, 101.4	3.89, ND[b]	ND, ND	ND, ND	ND. ND	ND, ND
	c	5.08, 101.4	3.91, ND	ND, ND	ND, ND	ND, ND	ND, ND
	d	5.11, 101.4	3.90, 77.8	ND, 71.4	ND, ND	ND, ND	ND, ND
t-α-Man*p*	(II) a	4.98, 102.4	3.77, 71.0	3.53, 72.1	3.71, 67.2	3.52, 73.1	3.73–3.70/3.55–3.49[a], 62.4
	b	4.96, 102.5	3.78, ND	3.53, 72.0	ND, ND	ND, 73.2	ND, ND
	c	4.92, 102.8	3.77, 71.0	3.51, 71.9	ND, ND	ND, 74.5	ND, ND
2,6-α-Man*p*	(III) a	4.84, 99.4	3.81, 77.8	3.72, 71.8	3.51, 68.4	3.49,74.2	3.50/3.92, 66.0
	b	4.86, 99.4	3.79, 78.6	ND, 71.6	ND, ND	3.51, ND	ND, ND
	c	4.87, 99.4	3.76, ND	ND, ND	ND, ND	ND, ND	ND, ND
6-α-Man*p*	(IV)	4.71, 99.4	3.72, 71.0	3.57, 72.0	ND, ND	ND, 73.0	ND, 66.7
α-Man*p*-2	(P3)	5.13, ~101.5	3.79, ND	ND, ND	ND, ND	ND, ND	ND, ND
	(P5)	5.13, ~101.5	3.81, ND	ND, ND	ND, ND	ND, ND	ND, ND
	(P6)	5.14, ~101.5	3.82, ND	ND, ND	ND, ND	ND, ND	ND, ND
	(P2)	5.14, ~101.5	3.80, ND	ND, ND	ND, ND	ND, ND	ND, ND
α-Man*p*-1	(P6)	5.15, ~101.3	3.61, ND	ND, ND	ND, ND	ND, ND	ND, ND
Myo-Ins	(P2)	3.95, ~76.9	4.21, ~78.8	3.22, ~71.2	3.43, ~73.8	3.08, ~74.9	3.63, 78.9
	(P3)	4.01, ~76.6	4.14, ~78.8	3.24, ~71.2	3.44, ~73.8	3.10, ~74.9	3.59, 80.8
	(P5)	4.01, ~76.6	4.18, ~78.8	3.24, ~71.2	3.44, ~73.8	3.11, ~74.9	3.60, 80.8
	(P6)	3.98, ~76.9	4.23, ~78.8	3.22, ~71.2	3.42, ~73.8	3.09, ~74.9	3.65, 78.9
Gro	(P2)	4.37/4.13, 63.4	5.12, 71.7	3.87/3.81, 63.5			
	(P3)	4.36/4.13, 63.4	5.12, 71.7	3.86/3.81, 63.5			
	(P5)	3.99, ND	ND, ND	3.81/3.76, ND			
	(P6)	3.98, ND	ND, ND	3.82/3.77, ND			

[a] The chemical shift of these protons could not be determined precisely and are given within an interval.
[b] ND, indicate that the chemical shift could not be determined.

Table I). According to the nomenclature used in our previous studies (43, 45), the phosphorus atoms at δ 1.83 and 1.85 corresponded to P2 and P3, respectively, defining an MPI anchor characterized by a diacylglycerol and a non-acylated *myo*-inositol. The phosphorus atom at δ 3.58 corresponded to P5, whereas that at δ 3.83 corresponded to an acyl-form not previously characterized and termed P6. P6 actually seems to be the equivalent of P2, yet in this case the MPI anchor bears a mono-acylated glycerol. Thus, both P5 and P6 MPI anchors are characterized by a 1-acyl-2-lysoglycerol and a non-acylated *myo*-inositol. The difference between acyl-forms P2 and P3 on one hand and P5 and P6 on the other most probably arises from the presence or lack of an additional fatty acid positioned on the Man*p* unit linked at *O*-2 of the *myo*-inositol.[2]

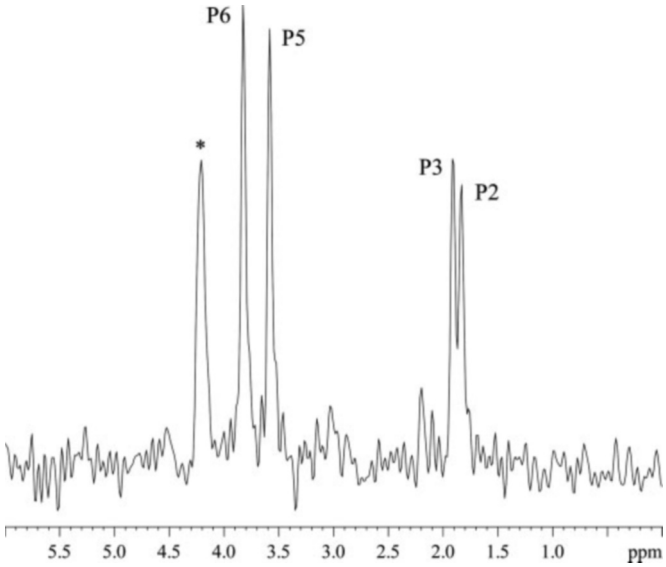

FIG. 4. **1D ^{31}P spectrum of SaeLM in Me_2SO-d6 at 343 K.** An expanded region (δ ^{31}P: 0.0–6.0) is shown. *, this signal does not correspond to a phosphate from a MPI anchor and was not present in all investigations.

The MPI anchor of mycobacterial lipoglycans is characterized by a *myo*-inositol unit glycosylated at position *O*-2 by a single Man*p* unit and at position *O*-6 by a Man*p* further glycosylated to give rise to the mannan core (1, 4). Man*p* units glycosylating the different *myo*-inositol units were defined thanks to ROESY experiment. Indeed, the *myo*-inositol protons H-2 at δ 4.14 (P3), 4.18 (P5), 4.21 (P2), and 4.23 (P6) showed intense nOe contacts with protons at δ 5.13, 5.13, 5.14, and 5.14, respectively, all tentatively attributed to mannosyl anomeric protons (Fig. 5*D*). This assumption was confirmed by the correlation of these protons on one hand with anomeric carbons at δ 101.5 on the ^{1}H-^{13}C HMQC spectrum (low intensity, not shown) and on the other hand with the H-2 protons at δ 3.79, 3.81, 3.80, and 3.82, respectively, on both the 2D ^{1}H-^{1}H HOHAHA (Fig. 3*C*) and ROESY (Fig. 3*D*) spectra. So, the Man*p* units defined by these chemical shifts corresponded to the Man*p* units glycosylating the *myo*-inositol ring at *O*-2 (labeled α-Man*p*-2 (43)), α-Man*p*-2 (P3), α-Man*p*-2 (P5), α-Man*p*-2 (P2), and α-Man*p*-2 (P6), respectively (Table I). In a similar way, the *myo*-inositol proton H-6 at δ 3.65 (P6) showed an intense nOe contact with a proton H-1 of a Man*p* unit at δ 5.15, correspond-

[2] M. Gilleron, J. Nigou, D. Nicolle, V. Quesniaux, and G. Puzo, submitted manuscript.

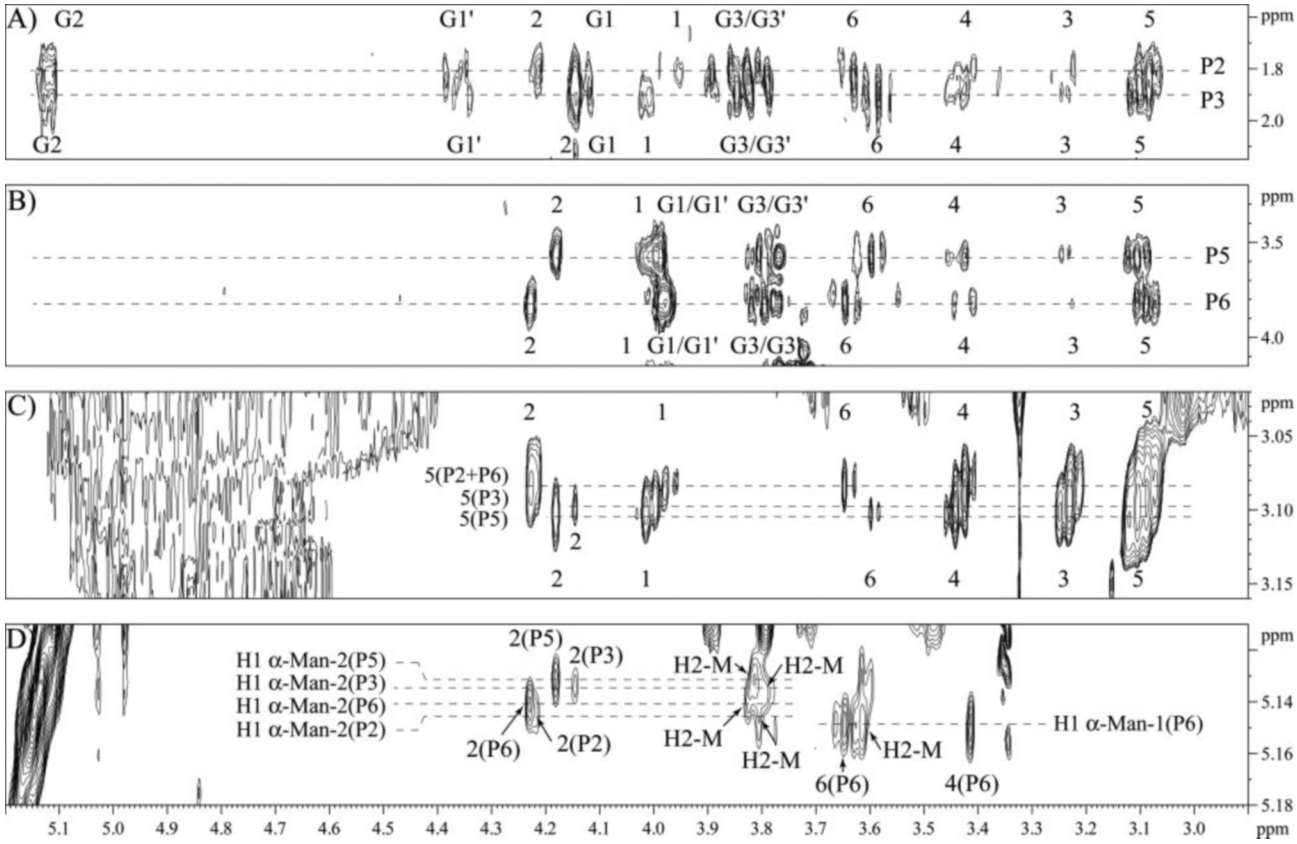

FIG. 5. **2D ^{1}H-^{31}P HMQC-HOHAHA τ_m 47 ms (*A* and *B*), 2D ^{1}H-^{1}H HOHAHA τ_m 110 ms (*C*), and ROESY τ_m 300 ms (*D*) spectra of SaeLM in Me_2SO-d6 at 343 K.** Expanded regions δ ^{1}H: 2.95–5.15, δ ^{31}P: 1.55–2.15 (*A*), δ ^{1}H: 2.95–5.15, δ ^{31}P: 3.20–4.15 (*B*), δ ^{1}H: 2.95–5.15, δ ^{1}H: 3.02–3.16 (*C*), and δ ^{1}H: 2.95–5.15, δ ^{1}H: 5.11–5.18 (D) are shown. *Numerals* correspond to the proton number of the *myo*-inositol units, and *numerals with letter G*, to the proton number of the glycerol units. Protons H-2 of mannosyl units are labeled *H2-M*. *α-Man-1*, α-Man*p* unit linked at *O*-6 of the *myo*-inositol; *α-Man-2*, α-Man*p* unit linked at *O*-2 of the *myo*-inositol.

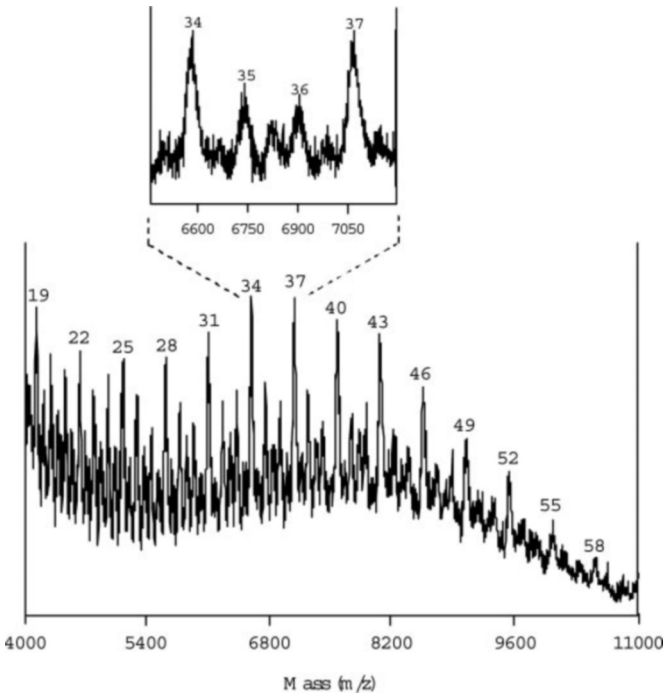

FIG. 6. **Negative MALDI-TOF mass spectrum of SaeLM.** 0.5 μl of a SaeLM solution at 10 μg/μl was mixed with 0.5 μl of the matrix solution (10 μg/μl of 2,5-dihydroxybenzoic acid in ethanol/water, 1:1, v/v) and analyzed by MALDI-TOF in the linear mode. The *number* on the *top* of each peak indicates the number of Man*p* units present on the corresponding main molecular species, *i.e.* tri-acylated.

ing to the Man*p* units glycosylating the *myo*-inositol ring at *O*-6, α-Man*p*-1 (P6). C-1 of Man*p*-1 (P6) was found to resonate at δ 101.3 on the ^{1}H-^{13}C HMQC spectrum (low intensity, not shown) and H-2 at δ 3.61 on the ^{1}H-^{1}H HOHAHA spectrum (Fig. 3*C*). H-1 of Man*p*-1 (P6) showed on the ^{1}H-^{1}H ROESY spectrum (Fig. 3*D*) intense contacts with its own H-2 at δ 3.61 and with the *myo*-inositol (P6) protons H-6 at δ 3.65, as indicated above, and with H-4 at δ 3.42 (Fig. 5*D*), but also much weaker nOe contacts with the *myo*-inositol (P6) H-1 at δ 3.98 and H-5 at δ 3.09 (not shown). No correlations with anomeric protons could be observed for proton H-6 of *myo*-inositol units corresponding to phosphorus P2, P3, or P5. However, as these protons are slightly more shielded than the H-6 of *myo*-inositol (P6), we cannot exclude that they might correlate with the H-1 of the same Man*p* unit, α-Man*p*-1 (P6), at δ 5.15, but the cross-peak might superimpose with that of the intra-residue α-Man*p*-1 H-1/H-2. Altogether, these data strongly indicated that SaeLM exhibits a MPI anchor similar to that of mycobacterial lipoglycans with a *myo*-inositol unit mannosylated at positions 2 and 6.

MALDI-TOF/MS Analysis—MALDI/MS analyses of mycobacterial LAM provided broad unresolved signals due to a complex heterogeneity of molecules differing in term of mannosylation, arabinosylation, and acylation (47). MS analyses of LAM are thus poorly informative, and an average molecular weight is the only information that can be deduced from the spectra. However, due to the lack of any arabinan domain, the mass distribution of LM molecules is still complex, although comparatively simpler as compared with that of LAM. Recently, MALDI/MS has proved to be much more efficient in analyzing LM molecules. Optimization of sample preparation and the choice of a suitable matrix enabled the recording of well resolved spectra resulting in ions corresponding to the different LM glyco- and acyl-forms.[2] Fig. 6 shows the linear negative mode MALDI mass spectrum of SaeLM using 2,5-dihydroxybenzoic acid, in a mixture water:ethanol (1/1, v/v) as a matrix. The spectrum is dominated by one major set of peaks, with a width of ~30 mass units, and separated by 486 mass units, predicting that the SaeLM major glyco-forms differ by three Man*p* residues. This observation is in total agreement with the structure deduced for the SaeLM mannan domain which corresponds to a polymer of trimannoside units. The peaks were assigned to deprotonated molecular ions $(M\text{-}H)^{-}$ typifying different glyco-forms of SaeLM. The distribution was centered on the peak centered at *m/z* 7075, tentatively attributed to a SaeLM glyco-form containing 37 Man*p* residues and an MPI anchor bearing three fatty acyl appendages, two hexadecanoic, and one octadecenoic acids, the main fatty acids detected by GC analysis. However, the width of 30 mass units observed for the peak could be explained by the presence of overlapping ions corresponding to less abundant mono-acylated species, containing either one hexadecanoic acid or one octadecenoic acid and 40 Man*p* units. In a similar way, the lowest molecular weight SaeLM glyco-forms recorded (Fig. 6) were in agreement with a tri-acylated species with 19 Man*p* residues or a mono-acylated species with 22 Man*p* residues. The highest molecular weight SaeLM glyco-forms were in agreement with a tri-acylated species with 58 Man*p* residues or a mono-acylated species with 61 Man*p* residues. So, this set of peaks characterized a tri-acylated acyl-form with a mannan domain composed of 19–58 α-D-Man*p* units and mono-acylated acyl-forms with a mannan domain composed of 22–61 α-D-Man*p* units. The distribution of glyco-forms was centered on the species containing 37 or 40 Man*p* units, which were also the most abundant species. Besides these major set of peaks, peaks with a lower intensity were recorded corresponding to the same acyl-forms that differed by 162 mass units corresponding to a difference of one Man*p* unit (see *inset* in Fig. 6). These species are likely to correspond to minor partially polymerized SaeLM glyco-forms. Altogether, these data allowed us to proposed the structural model depicted in Fig. 7.

TNF-α Production by Macrophages—The potency of SaeLM to stimulate the production of TNF-α was investigated using human THP-1 monocyte cell lines. SaeLM, when tested at concentrations of 10 and 20 μg/ml, induced a strong dose-dependent production of TNF-α (Fig. 8*A*), which was not inhibited by polymyxin B (not shown), indicating that the observed cytokine induction was not due to LPS contamination. In contrast, mycobacterial ManLAM, known to be a poor inducer of pro-inflammatory cytokines, induced a very weak amount of TNF-α.

It has been previously demonstrated that mycobacterial LM and PIM stimulate the production of TNF-α in a TLR-2-dependent fashion (16, 48). To investigate the TLR dependence of TNF-α-inducing SaeLM activity, studies were conducted by measuring the inhibitory effect of cytokine production using specific anti-TLR-2 and anti-TLR-4 antibodies. As shown in Fig. 8*B*, whereas the anti-TLR-4 and an IgG2 isotype control antibodies had no affect on TNF-α production induced by SaeLM, the anti-TLR-2 antibody inhibited this production. These data clearly underscore the role of TLR-2 in mediating the stimulation of TNF-α production by THP-1 cells in response to SaeLM.

To gain better insights into the structure/function relationships, SaeLM activity was compared with that of *M. bovis* BCG LM (BCGLM) and TpaLAM lipomannan core (mahTpaLAM), both known to exhibit a pro-inflammatory activity. When tested at the same concentrations (10 and 20 μg/ml), SaeLM was found to exhibit a stronger TNF-α-inducing activity than BCGLM, the latter being more active than mahTpaLAM (Fig. 8*A*). These data confirm that the presence of an (α1→6)-Man*p* chain is sufficient in providing pro-inflammatory activity for

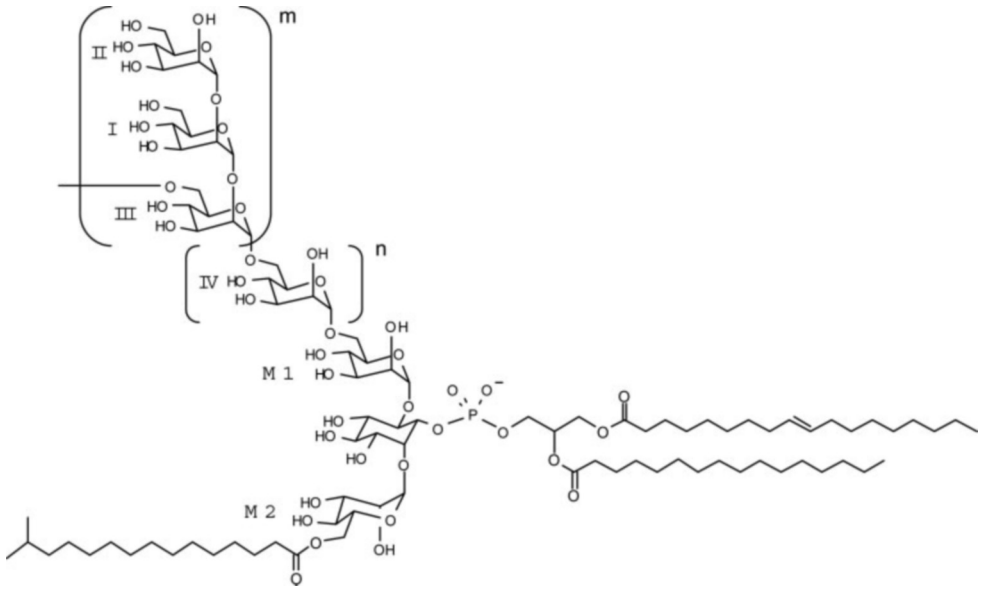

FIG. 7. **Structural model of SaeLM.** SaeLM contained an MPI anchor glycosylated by a (α1→6)-Man*p* chain, which is further substituted, as indicated by integration of anomeric protons signals, at 83% (on average) of the *O*-2 positions by side chains composed of the Man*p*-(α1→2)-Man*p*-(α1→ motif. MALDI/MS analysis showed that SaeLM was composed of a mixture of glyco-forms containing 19–61 Man*p* units. The distribution of glyco-forms was centered on the species containing 37 or 40 Man*p* units. The branched and linear portions of the (α1→6)-Man*p* chain form distinct domains. The tri-acylated MPI anchor drawn, characterized by phosphate P3, corresponds to one of the SaeLM acyl-forms. *m* and *n* can be estimated on average at 11 and 2, respectively. The nature of the fatty acids (iC16:0, C16:0, and C18:1) is in agreement with the GC data; however, their relative distribution on the different acylation sites is unknown. *M1*, α-Man-1; *M2*, α-Man-2.

LM-like molecules as observed for mahTpaLAM. However, the presence of side chains, depending on their length and degree of sophistication, increases this activity. Nevertheless, one should not neglect the acylation pattern that might also influence the relative activity of these LM-like molecules,[2] because deacylated SaeLM (dSaeLM), obtained after an alkaline treatment, was unable to induce TNF-α (Fig. 8*A*).

DISCUSSION

LM-like molecules are powerful pro-inflammatory lipoglycans found in the cell wall of mycobacteria and some of the related actinomycetes genera, however the structure/function relationships underlying their activity are not fully understood. Nevertheless, it is now established that the intrinsic capacity of lipoglycans to induce a TLR-2-dependent production of pro-inflammatory cytokines derives from the lipomannan core of the molecule and that this activity is reduced when the lipomannan core is sterically masked by a significant arabinan domain. This has been clearly demonstrated with lipoglycans from *Mycobacterium kansasii* (16) and *T. paurometabola* (22). Indeed the LAM of these species exhibits a poor activity; however, upon chemical degradation of the arabinan domain by mild acid hydrolysis, the resulting lipomannan moiety elicits a powerful pro-inflammatory response with a magnitude similar to that of "free" LM. However, mycobacterial LM is a heterogeneous mixture, and the precise structural basis of the interaction with the receptor still remains obscure. Chemical synthesis of LM-like molecules can be hardly envisaged. So, further insights into deciphering these complex molecular interactions could benefit from the fine structural and functional characterizations of lipoglycan variants. Indeed, various actinomycetes species (31) offer the opportunity to study lipoglycans with a high molecular diversity that can be utilized to refine structure/function relationships.

In this context, we report here the isolation and the structural and functional characterization of a new LM variant in the *Pseudonocardineae*, *S. aerocolonigenes* (31). The investigation revealed an original structure, and furthermore, we demonstrate that the LM possessed potent pro-inflammatory activity. SaeLM contained mannose as the sole carbohydrate. The main fatty acids esterifying SaeLM are 14-methylpentadecanoic, palmitic, and octadecenoic acids in agreement with the fatty acid composition found in the *Saccharothrix* genus (49). Per-*O*-methylation and detailed NMR studies revealed that SaeLM was composed from a (α1→6)-Man*p* chain, which is further substituted at more than 80% of the *O*-2 positions by side chains composed of the Man*p*-(α1→2)-Man*p*-(α1→ motif (Fig. 7). The structure of this mannan core, containing dimannoside side chains, is in contrast with that of mycobacterial LM where only single mannopyranosyl units substitute the (α1→6)-Man*p* chain (4), except in a clinical isolate of *M. kansasii* where the LM has been reported to contain very few dimannoside side chains (50). Interestingly, some discrete trimannoside motifs, defined by spin systems Id, IIc, and IIIb, were identified and are probably located at a particular site in the structure, such as the beginning or the end of the chain. As previously stated the mannan domain of LM molecules is composed of a (α1→6)-Man*p* chain substituted at some *O*-2 or *O*-3 positions by lateral side chains. On mycobacterial LM, one unanswered question remains: whether the linear and branched portions of the mannan core form distinct domains or whether 2,6-α-Man*p* and 6-α-Man*p* units intercalate at frequent regular intervals within the chain. In the case of SaeLM we found that proton H-1 of these two units correlated with their own C-6 resonances in the HMBC spectrum, and furthermore were distinguishable (Fig. 2*C*). Altogether, this suggests that 2,6-α-Man*p* on one hand, and 6-α-Man*p* units on the other hand, are interconnected and consequently form distinct domains.

1D ^{31}P NMR analysis of SaeLM showed that the MPI anchor contained four acyl-forms, with a significant predominance of mono-acylglycerol (62%) as compared with di-acylglycerol (38%) acyl-forms. This distribution is in contrast with the data on *M. tuberculosis* or *M. bovis* BCG lipoglycans where the acyl-forms bearing diacylglycerols are the most abundant. In addition, position 3 of the *myo*-inositol was not acylated. Acylation of *myo*-inositol on lipoglycans actually seems to be re-

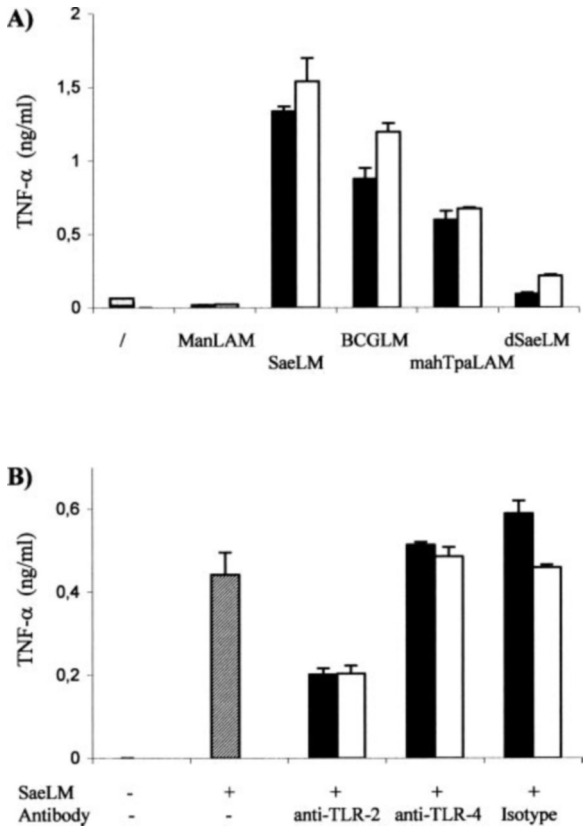

FIG. 8. **TNF-α production by human THP-1 monocyte/macrophage cell line in response to SaeLM and various stimuli.** *A*, ManLAM, SaeLM, BCGLM, mahTpaLAM, or dSaeLM were tested at 10 (*black bars*) and 20 (*white bars*) μg/ml. Polymixin B, when previously added, had no effect on the amount of TNF-α released by these stimuli (not shown). LPS from *E. coli* 055:B5, at a concentration of 0.2 μg/ml, induced 1020 pg/ml TNF-α. *B*, TLR dependence of SaeLM pro-inflammatory activity. SaeLM at 10 μg/ml and the various antibodies (anti-TLR-2, anti-TLR-4, and IgG2 isotype control) at a concentration of 10 (*black bars*) or 20 (*white bars*) μg/ml were added to THP-1 cells. LPS at a concentration of 0.2 μg/ml induced 510 pg/ml TNF-α. ManLAM and LM were from *M. bovis* BCG; mahTpaLAM was prepared as previously described (22). *BCGLM*, LM from *M. bovis* BCG; *dSaeLM*, deacylated SaeLM; *mahTpaLAM*, mild acidic hydrolyzed TpaLAM, *i.e.* TpaLAM lipomannan core.

stricted to the *Mycobacterium* genus, because it was not observed in any of the lipoglycans investigated so far arising from the genera, *Rhodococcus* (25, 26), *Tsukamurella* (22), *Amycolatopsis* (28), or *Turicella* (30). These findings are surprising because acylation of *myo*-inositol was, at least, observed on PIM, in *Rhodococcus equi* (25). This suggests that there is a different fatty acid modeling system in mycobacteria compared with the other actinomycetes genera. However it has been shown that mycobacterial lipoglycan biosynthesis occurs mainly from tri-acylated PIM precursors (6, 51, 52). Moreover, position *O*-3 of *myo*-inositol is the last one to be acylated during biosynthesis (48, 53), and as such, tetra-acylated forms of PIMs may constitute a storage pool of PIMs. MPI anchors corresponding to P2 and P3 on one hand and P5 and P6 on the other hand do not show, as revealed by 2D ^{1}H-^{31}P HMQC-HOHAHA, any difference in terms of acylation of the *myo*-inositol and the glycerol units. The difference probably arises from the acylation state of the fourth potential acylation site of the MPI anchor that cannot be investigated by this approach, *i.e.* position 6 of the Man*p* unit linked at *O*-2 of the *myo*-inositol (1, 4). Indeed it has been found, after purification of the individual acyl-forms of *M. bovis* BCG LM and analysis by MALDI-MS that P2 and P3 MPI differ by the presence of an additional fatty acid, with P3 containing the additional fatty acid.[2] In a similar way, P6 defined in the present study, which seems actually to be the equivalent of P2, is likely to differ from P5 by the absence of a fatty acid on the Man*p* unit, because P5 has been shown to bear one in this position.[2] SaeLM MPI anchor was found to be based on a diglycosylated *myo*-inositol unit substituted at positions *O*-2 and *O*-6, by a t-Man*p* unit and the mannan core, respectively. Indeed the Man*p* units glycosylating the *myo*-inositol were clearly identified by NMR experiments. H-1 of α-Man*p*-1 (linked at *O*-6 of *myo*-inositol) and of α-Man*p*-2 (linked at *O*-2 of *myo*-inositol) units were deshielded as compared with the other carbohydrate anomeric resonances and consequently could be detected despite their low abundance. They were clearly identified on the ROESY spectrum due to intense nOe contacts between their H-1 and H-2 or H-6 of *myo*-inositol, respectively (Fig. 5). The different anomeric protons of α-Man*p*-2 units corresponding to the acyl-forms characterized by the phosphates P2, P3, P5, and P6 could be readily distinguished. However the anomeric protons of the different α-Man*p*-1 units may overlap.

MALDI/MS, after optimization of sample preparation and recording conditions as well as the choice of a suitable matrix, has recently been shown to be a suitable method for analyzing the molecular distribution of *M. bovis* BCG LM, in terms of glyco- and acyl-forms.[2] MALDI/MS spectra of SaeLM showed a major set of peaks with a width of around 30 mass units (Fig. 6). They were attributed to a superimposition of ions corresponding to species bearing an MPI anchor containing either one or three fatty acyl groups. However, these results failed to reveal the heterogeneity of SaeLM acyl-forms, as shown by ^{31}P NMR. This is due mainly to the suppressive effects of MS experimentation that preclude one from obtaining spectra that would reflect the real abundance of the different acyl-forms, which has recently been observed with mycobacterial LM.[2] Nevertheless, MS analysis indicated that SaeLM was composed of a mixture of glyco-forms containing 19–61 Man*p* units. The distribution of glyco-forms was centered on the species containing 37 or 40 Man*p* units. SaeLM appears to be larger in size than *M. bovis* BCG LM, which shows a distribution of glyco-forms of 15–45 Man*p* units, being centered on the species containing 26 Man*p* units.[2] However, SaeLM possesses a (α1→6)-Man*p* chain (average of 14 units) with a size similar to that of *M. bovis* BCG LM. This results from the fact that SaeLM exhibits dimannoside side chains instead of single t-Man*p* units for *M. bovis* BCG LM (43).

In summary, SaeLM exhibits an original structure with the same core domains as described for mycobacterial LM, but with some differences in acylation, branching, and size of the side chains present on the mannan core. Altogether SaeLM, with dimannoside side chains, appears to be the most elaborated non-mycobacterial LM molecule identified to date (Fig. 7).

LM (16–18) and lipomannan-domain-containing molecules (22) possess conserved structural motifs that are able to induce pro-inflammatory activity, however, in order for optimal induction, this structural moiety must be readily accessible to the host receptor(s). Interestingly, TpaLAM lipomannan core (mahTpaLAM), composed of an (α1→6)-Man*p* chain with no side chains, is a powerful inducer of TNF-α, demonstrating that an (α1→6)-Man*p* chain is sufficient in providing pro-inflammatory activity and that branched t-Man*p* units are not necessarily required. LM-like molecules activate immune cell responses via TLR-2; however, the molecular dynamics of LM-like molecules binding to TLR-2, in particular, and in general of TLR ligands binding to their receptor(s) remains unclear (54). Accessory molecules such as LBP or CD14 (16) or heterodimerization with another TLR such as TLR-1 (55) participate in the recognition process of LM. Nevertheless, a direct interaction

between the pathogen-associated molecular patterns and TLR-2 receptor has been clearly shown to be involved in signaling (56). Here we found that SaeLM exhibited a stronger TNF-α-inducing activity than *M. bovis* BCG LM, the latter being more active than mahTpaLAM. Altogether these data establish that a linear (α1→6)-Man*p* chain, linked to the MPI anchor, is sufficient in providing pro-inflammatory activity. However adding side chains and extending their size increases this activity, most probably as a result of a higher affinity for TLR-2. In addition, the acylation pattern might also influence the relative activity of these LM-like molecules, because deacylated SaeLM (dSaeLM), obtained after an alkaline treatment, was unable to induce TNF-α. Altogether, our findings provide better understanding of the structure/function relationship of TLR-2 lipoglycan-dependent signaling. In addition, and of more general interest, this study participates in the effort of deciphering the molecular basis of the recognition of pathogen-associated molecular patterns by TLRs.

Acknowledgment—We gratefully acknowledge Thérèse Brando (Institut de Pharmacologie et de Biologie Structurale, Toulouse) for expert technical assistance with capillary electrophoresis/laser-induced fluorescence experiments.

REFERENCES

1. Chatterjee, D., and Khoo, K. H. (1998) *Glycobiology* **8,** 113–120
2. Gilleron, M., Rivière, M., and Puzo, G. (2001) in *Glycans in Cell Interaction and Recognition: therapeutic Aspects* (Aubery, M., ed) pp. 113–140, Harwood Academic Press, Amsterdam
3. Nigou, J., Gilleron, M., Rojas, M., Garcia, L. F., Thurnher, M., and Puzo, G. (2002) *Microbes Infect.* **4,** 945–953
4. Nigou, J., Gilleron, M., and Puzo, G. (2003) *Biochimie* (*Paris*) **85,** 153–166
5. Briken, V., Porcelli, S. A., Besra, G. S., and Kremer, L. (2004) *Mol. Microbiol.* **53,** 391–403
6. Besra, G. S., Morehouse, C. B., Rittner, C. M., Waechter, C. J., and Brennan, P. J. (1997) *J. Biol. Chem.* **272,** 18460–18466
7. Knutson, K. L., Hmama, Z., Herrera-Velit, P., Rochford, R., and Reiner, N. E. (1998) *J. Biol. Chem.* **273,** 645–652
8. Nigou, J., Zelle-Rieser, C., Gilleron, M., Thurnher, M., and Puzo, G. (2001) *J. Immunol.* **166,** 7477–7485
9. Geijtenbeek, T. B., Van Vliet, S. J., Koppel, E. A., Sanchez-Hernandez, M., Vandenbroucke-Grauls, C. M., Appelmelk, B., and Van Kooyk, Y. (2003) *J. Exp. Med.* **197,** 7–17
10. Tailleux, L., Maeda, N., Nigou, J., Gicquel, B., and Neyrolles, O. (2003) *Trends Microbiol.* **11,** 259–263
11. Gilleron, M., Himoudi, N., Adam, O., Constant, P., Venisse, A., Riviere, M., and Puzo, G. (1997) *J. Biol. Chem.* **272,** 117–124
12. Adams, L. B., Fukutomi, Y., and Krahenbuhl, J. L. (1993) *Infect. Immun.* **61,** 4173–4181
13. Means, T. K., Lien, E., Yoshimura, A., Wang, S., Golenbock, D. T., and Fenton, M. J. (1999) *J. Immunol.* **163,** 6748–6755
14. Guerardel, Y., Maes, E., Elass, E., Leroy, Y., Timmerman, P., Besra, G. S., Locht, C., Strecker, G., and Kremer, L. (2002) *J. Biol. Chem.* **277,** 30635–30648
15. Barnes, P. F., Chatterjee, D., Abrams, J. S., Lu, S., Wang, E., Yamamura, M., Brennan, P. J., and Modlin, R. L. (1992) *J. Immunol.* **149,** 541–547
16. Vignal, C., Guerardel, Y., Kremer, L., Masson, M., Legrand, D., Mazurier, J., and Elass, E. (2003) *J. Immunol.* **171,** 2014–2023
17. Quesniaux, V. J., Nicolle, D. M., Torres, D., Kremer, L., Guerardel, Y., Nigou, J., Puzo, G., Erard, F., and Ryffel, B. (2004) *J. Immunol.* **172,** 4425–4434
18. Dao, D. N., Kremer, L., Guerardel, Y., Molano, A., Jacobs, W. R., Jr., Porcelli, S. A., and Briken, V. (2004) *Infect. Immun.* **72,** 2067–2074
19. Heldwein, K. A., Liang, M. D., Andresen, T. K., Thomas, K. E., Marty, A. M., Cuesta, N., Vogel, S. N., and Fenton, M. J. (2003) *J. Leukoc. Biol.* **74,** 277–286
20. Heldwein, K. A., and Fenton, M. J. (2002) *Microbes Infect.* **4,** 937–944
21. Basu, S., and Fenton, M. J. (2004) *Am. J. Physiol.* **286,** L887–L892
22. Gibson, K. J., Gilleron, M., Constant, P., Brando, T., Puzo, G., Besra, G. S., and Nigou, J. (2004) *J. Biol. Chem.* **279,** 22973–22982
23. Sidobre, S., Nigou, J., Puzo, G., and Riviere, M. (2000) *J. Biol. Chem.* **275,** 2415–2422
24. Sidobre, S., Puzo, G., and Riviere, M. (2002) *Biochem. J.* **365,** 89–97
25. Garton, N. J., Gilleron, M., Brando, T., Dan, H. H., Giguere, S., Puzo, G., Prescott, J. F., and Sutcliffe, I. C. (2002) *J. Biol. Chem.* **277,** 31722–31733
26. Gibson, K. J., Gilleron, M., Constant, P., Puzo, G., Nigou, J., and Besra, G. S. (2003) *Microbiology* **149,** 1437–1445
27. Flaherty, C., and Sutcliffe, I. C. (1999) *Syst. Appl. Microbiol.* **22,** 530–533
28. Gibson, K. J., Gilleron, M., Constant, P., Puzo, G., Nigou, J., and Besra, G. S. (2003) *Biochem. J.* **372,** 821–829
29. Sutcliffe, I. C. (1995) *Arch. Oral. Biol.* **40,** 1119–1124
30. Gilleron, M., Garton, N. J., Nigou, J., Brando, T., Puzo, G., and Sutcliffe, I. C. (2005) *J. Bacteriol.* **187,** 854–861
31. Stackebrandt, E., Rainey, F. A., and Ward-Rainey, N. L. (1997) *Int. J. Syst. Bacteriol.* **47,** 479–491
32. Labeda, D. P., Hatano, K., Kroppenstedt, R. M., and Tamura, T. (2001) *Int. J. Syst. Evol. Microbiol.* **51,** 1045–1050
33. Nigou, J., Gilleron, M., Cahuzac, B., Bounery, J. D., Herold, M., Thurnher, M., and Puzo, G. (1997) *J. Biol. Chem.* **272,** 23094–23103
34. Ludwiczak, P., Gilleron, M., Bordat, Y., Martin, C., Gicquel, B., and Puzo, G. (2002) *Microbiology* **148,** 3029–3037
35. Ciucanu, I., and Kerek, F. (1984) *Carbohydr. Res.* **131,** 209–217
36. Shaka, A. J., Barker, P. B., and Freeman, R. (1985) *J. Magn. Reson.* **64,** 547–552
37. Bax, A., and Subramanian, S. (1986) *J. Magn. Reson.* **67,** 565–569
38. Bax, A., and Summers, M. F. (1986) *J. Am. Chem. Soc.* **108,** 2093–2094
39. Lerner, L., and Bax, A. (1986) *J. Magn. Reson.* **69,** 375–380
40. Bax, A., and Davies, D. G. (1985) *J. Magn. Reson.* **65,** 355–360
41. Bax, A., and Davis, D. G. (1985) *J. Magn. Reson.* **63,** 207–213
42. Gilleron, M., Bala, L., Brando, T., Vercellone, A., and Puzo, G. (2000) *J. Biol. Chem.* **275,** 677–684
43. Gilleron, M., Nigou, J., Cahuzac, B., and Puzo, G. (1999) *J. Mol. Biol.* **285,** 2147–2160
44. Bock, K., and Pedersen, C. J. (1974) *J. Chem. Soc. Perkin Transac.* **2,** 293
45. Nigou, J., Gilleron, M., and Puzo, G. (1999) *Biochem. J.* **337,** 453–460
46. Bosco, M., Culeddu, N., Toffanin, R., and Pollesello, P. (1997) *Anal. Biochem.* **245,** 38–47
47. Venisse, A., Berjeaud, J. M., Chaurand, P., Gilleron, M., and Puzo, G. (1993) *J. Biol. Chem.* **268,** 12401–12411
48. Gilleron, M., Quesniaux, V. F., and Puzo, G. (2003) *J. Biol. Chem.* **278,** 29880–29889
49. Lee, S. D., Kim, E. S., Roe, J. H., Kim, J., Kang, S. O., and Hah, Y. C. (2000) *Int. J. Syst. Evol. Microbiol.* **50,** 1315–1323
50. Guerardel, Y., Maes, E., Briken, V., Chirat, F., Leroy, Y., Locht, C., Strecker, G., and Kremer, L. (2003) *J. Biol. Chem.* **278,** 36637–36651
51. Takayama, K., and Goldman, D. S. (1969) *Biochim. Biophys. Acta* **176,** 196–198
52. Kremer, L., Gurcha, S. S., Bifani, P., Hitchen, P. G., Baulard, A., Morris, H. R., Dell, A., Brennan, P. J., and Besra, G. S. (2002) *Biochem. J.* **363,** 437–447
53. Gilleron, M., Ronet, C., Mempel, M., Monsarrat, B., Gachelin, G., and Puzo, G. (2001) *J. Biol. Chem.* **276,** 34896–34904
54. Bell, J. K., Mullen, G. E., Leifer, C. A., Mazzoni, A., Davies, D. R., and Segal, D. M. (2003) *Trends Immunol.* **24,** 528–533
55. Tapping, R. I., and Tobias, P. S. (2003) *J. Endotoxin. Res.* **9,** 264–268
56. Iwaki, D., Mitsuzawa, H., Murakami, S., Sano, H., Konishi, M., Akino, T., and Kuroki, Y. (2002) *J. Biol. Chem.* **277,** 24315–24320